Review Article

New developments in treatment planning and verification of particle beam therapy

Reinhard W. Schulte, Andrew J. Wroe

Department of Radiation Medicine, Translational Research, Loma Linda University Medical Center, Loma Linda, CA, 92354, USA
Corresponding to: Reinhard W. Schulte, M.D, M.S. 11234 Anderson St., Loma Linda, CA 92354, USA. Email: rschulte@llu.edu.

Abstract: Charged particle beam therapy has been used for almost 60 years. During the initial 40 years, the medical use of protons and heavy ions was explored at accelerator laboratories in a limited number of patients and for a limited number of cancerous and non-cancerous disease conditions. After the development of computed tomography and 3D treatment planning, it was time to move charged particle therapy into the clinical realm. This happened in October 1991 when an ocular melanoma patient became the first patient to be treated at Loma Linda University Medical Center in California. Due to the increased awareness of the advantages of charged particle therapy and promising results of single-institution experiences, one currently observes a phase of rapid expansion of proton treatment centers throughout the world. A few of these centers are combined proton/carbon ion facilities. It is very important that the technological evolution of charged particle therapy will continue during this phase of clinical expansion to ensure that the increasing number of patients exposed to therapeutic charged particles will benefit most from the advantageous dose distributions that these particles afford. This report will give an overview of translational research activities related to planning and verification of proton therapy in which the authors have been involved for a number of years. While our activities focus on protons, these developments are to a large degree also applicable to carbon ion therapy.

Key Words: Proton therapy; proton computed tomography; range verification; immobilization

Submitted Sep 22, 2012. Accepted for publication Oct 23, 2012.
DOI: 10.3978/j.issn.2218-676X.2012.10.07
Scan to your mobile device or view this article at: http://www.thetcr.org/article/view/598/html

Introduction

Proton therapy is currently expanding its role in radiation therapy. In the U.S., there are at present 10 clinical proton treatment facilities, with 9 centers operating proton gantries, and 7 additional facilities in the planning and construction phase (1). Charged-particle beams heavier than electrons, including protons, helium and carbon ions, are distinguished from photon beams by the unique property of dose deposition at a precise depth, known as the Bragg peak, with a steep dose falloff beyond the peak. Thus, the integral dose to surrounding normal tissues is generally less compared with photon radiation therapy. Having fine control over the dose deposition in the patient allows for generation of very conformal dose distributions. Sparing of critical normal structures and minimizing integral dose to normal tissues appears most advantages in the central nervous system (CNS), where critical structures are densely packed and often abutted by gross tumor, and in children whose normal brain is very radiosensitive and who are at the highest risk of developing secondary cancers.

The wide-spread use of proton therapy in other body sites, in particular in prostate cancer, where it is in fact used most often, is currently controversial because no clear benefit over intensity modulated radiation therapy (IMRT) with photons has been demonstrated (2). While head-to-head trials comparing IMRT and proton therapy may be conducted in prostate cancer patients in the near future, where the wide use of proton therapy is most controversial, one should keep in mind that proton therapy is far from fully developed. Range uncertainties in proton therapy

© Pioneer Bioscience Publishing Company. All rights reserved.

that are amplified in body treatment sites due to material heterogeneity, organ deformation and internal motion can negatively impact the delivered dose distribution and are the subject of ongoing study and improvements. Closely related to this subject is the continued development of image guidance technology in the treatment room that ideally will provide feedback for in-room treatment plan modifications (adaptive proton therapy). It appears that full implementation of inversely planned intensity modulated proton beam therapy (IMPBT) with all its advantages will have to await these developments.

A related and often overlooked subject of interest in proton and heavy ion therapy is the immobilization of the patient. For the various anatomic sites, specific devices have to be developed that position and immobilize the patient reproducibly and effectively. In charged particle therapy, attention needs to be paid to minimize the proton water equivalent thickness (WET) of the immobilization devices in order to reduce the effect on proton beam penumbra and range uncertainty.

The next major step in therapeutic proton beam technology is to supplement passive beam delivery and shaping techniques with active proton beam scanning techniques. Proton beam scanning is currently being developed and implemented at major academic proton treatment centers. The major advantage of proton beam scanning as compared to passive beam delivery methods is the ability to perform inversely planned and optimized IMPBT. However, there are major technological hurdles to be overcome with proton beam scanning. In fact, most existing proton treatment centers continue to employ passive scattering systems.

In this contribution, the authors give an overview on developments undertaken by the translational medical physics and technology team at the James M. Slater Proton Treatment and Research Center at Loma Linda University Medical Center (LLUMC) to overcome some of the technical and conceptual hurdles currently encountered in proton and heavy ion therapy. While our developments are specifically geared towards improving proton therapy, they can be equally applied to heavy ion therapy.

Concepts and strategies

The classical strategy of planning and delivering a radiation treatment is to first scan the patient with X-ray computed tomography (CT) and to define the gross tumor and clinical target volumes (GTV and CTV) and organs at risk (OARs) with support of registered complementary imaging studies. At the time of the planning CT scan, the patient has been provided with appropriate immobilization support, and the position during the planning CT needs to be reproduced later in the treatment room.

Reproduction of the planned patient position and distribution of tissues relative to the beam is very important in proton therapy. Slight changes in the distribution of tissues relative to the beam due to setup errors, differences between the immobilization devices used during planning and treatment, and interim changes in patient or tumor anatomy, e.g., due to tumor shrinkage or weight changes, can have a noticeable influence on the resulting dose distribution at the time of treatment. Some of these uncertainties are random (e.g., variations in patient position); however, others, such as tumor shrinkage and weight loss or gain, are systematic and, therefore, may lead to a significant underdosing of tumor and overdosing of organs at risk since the range of the charged particle beams has changed compared to the original plan. This situation is further complicated when tumor sites are characterized by significant organ motion and deformation, such as intra-abdominal tumors, lung tumors, breast tumors, and even prostate tumors since the position of the prostate is influenced by the filling of bladder, rectum and small bowel. Uncertainties in range due to intra- and interfractional target motion can significantly modify the proton beam dose distribution and lead to cold spots and hot spots (3).

All the systematic and random errors combined require a considerable lateral margin to be added to the CTV to derive the internal target volume (ITV) and planning target volume (PTV). While this is also true in photon therapy, such as IMRT, distal uncertainty margins due to range errors are unique to charged particle therapy and are specific to each beam.

Organ motion is less of an issue in CNS and head and neck sites. However, there are considerable range uncertainties due to the presence of considerable bone and air inhomogeneity, CT artifacts from dental fillings, and tissue or tumor changes during the course of the treatment (e.g., in intra-orbital tumors or head and neck carcinomas).

The presence of range uncertainty in charge particle therapy has been known for a long time, and has been addressed in many ways, with the ultimate goal to reduce them to the fullest extent possible. Monte Carlo (MC) studies have been used to show the effect of inaccuracies resulting from conversion of Hounsfield units to relative stopping power (RSP) with respect to water in

© Pioneer Bioscience Publishing Company. All rights reserved.

analytical dose calculations as well as MC-based dose algorithms (4-6). A recent study, utilizing the change of bone marrow fat signal in MRI after proton treatment, demonstrated the range uncertainty encountered in posterior spinal proton fields in 10 patients (7). The mean overshoot was 1.9 mm (95% confidence interval, 0.8-3.1 mm) and exceeded 3 mm in four patients. In addition, there have been attempts to develop robust treatment planning algorithms that optimize beam direction to minimize range uncertainty (8-10).

At LLUMC, we have chosen to invest in the development of proton CT (pCT) as a promising technique to reduce systematic uncertainties in RSP determination related to the Hounsfield unit conversion (see below). Another interesting approach is the development of dual-energy CT scanners, which may provide better RSP estimates than single-energy CT scans (11). Yet the development of pCT presents additional advantages for proton therapy. One such advantage is the ability to provide similar or even better images with fewer artifacts than X-ray cone beam CT, making pCT useful for not only treatment planning but also pretreatment monitoring of patent setup. Besides cross-sectional anatomy, the pre-treatment pCT study also provides the RSP distribution of the patient and, in combination with fast computational hardware, may be able to check the adequacy of the treatment before its delivery, or even modify beam angles to optimize the treatment delivery. We currently have no data that supports these applications, but one should consider this for future research and development once pCT technology has been fully translated into clinical application.

While we were studying the application of radiation detectors typically employed in high-energy physics research, i.e., particle trackers and energy/range detectors (calorimeters), for proton CT, it became apparent that these detectors can also be used to monitor the proton radiation delivery by detecting primary or secondary particles generated during beam delivery. This led to the investigation of interaction vertex and proton scattering imaging during pencil beam scanning of charged particle beams, which will also be discussed below.

Lastly, one needs to pay meticulous attention to the immobilization devices that are used during CT scanning and treatment. Special immobilization devices for proton therapy have been developed that help to minimize additional range uncertainties and beam widening due to scattering. The importance of implementation of such devices will also be addressed in this contribution.

Proton CT

The standard approach to deal with range uncertainties in charged particle therapy is to add an additional range to each beam according to the expected range uncertainty, assuring target volume coverage (12). However, this can lead to unsatisfactory results by over-treating normal tissues. Initially, CT units used in charged particle treatment planning were calibrated with standard tissue substitutes (13). Schneider *et al.* (14) showed that this method is very sensitive to the choice of tissue substitutes and can lead to maximum range errors in the head in excess of 20 mm. These investigators developed a "stoichiometric calibration" method (15), which is based on data published in ICRP report 44 (16) for the calculation of Hounsfield values and RSP power. This is done after the dependence of the particular CT scanner on atomic composition has been measured with tissue substitutes. The stoichiometric method does not solve the problem that tissues of the same Hounsfield values can have different RSP. Schneider *et al.* (17) also showed that the "best" CT calibration was achieved when the CT of an individual patient was calibrated with proton radiography, which provides a composite "projection" image of integral RSP in proton beam direction. While this work pointed to the usefulness of RSP measurements as the basis for quality assurance of X-ray-CT-based charged particle treatment planning, it did not make the innovative step towards using protons themselves for CT planning.

Proton CT itself is not a new idea. It was originally suggested by Alan Cormack (18), who shared the Nobel Prize with Hounsfield for his seminal work on CT image reconstruction. He mentioned proton CT in his original paper as well as in his Nobel lecture (19). Driven by the clinical need for more proton range accuracy, a scientific pCT collaboration was formed by investigators from the Department of Radiation Medicine at LLUMC, University of California Santa Cruz (UCSC) (20), Brookhaven National Laboratory (BNL), and the State University of New York Stony Brook in 2003. A series of publications appeared during this exploratory (and mostly unfunded) period of 2003-2008 (21-27), documenting progress made in the conceptual and scientific understanding of the new pCT technology and pCT reconstruction.

The recent development of pCT has mostly become possible by application of the latest detector technology adapted from High Energy Physics (HEP). Silicon microstrip trackers and crystal calorimetry, commonly

© Pioneer Bioscience Publishing Company. All rights reserved.

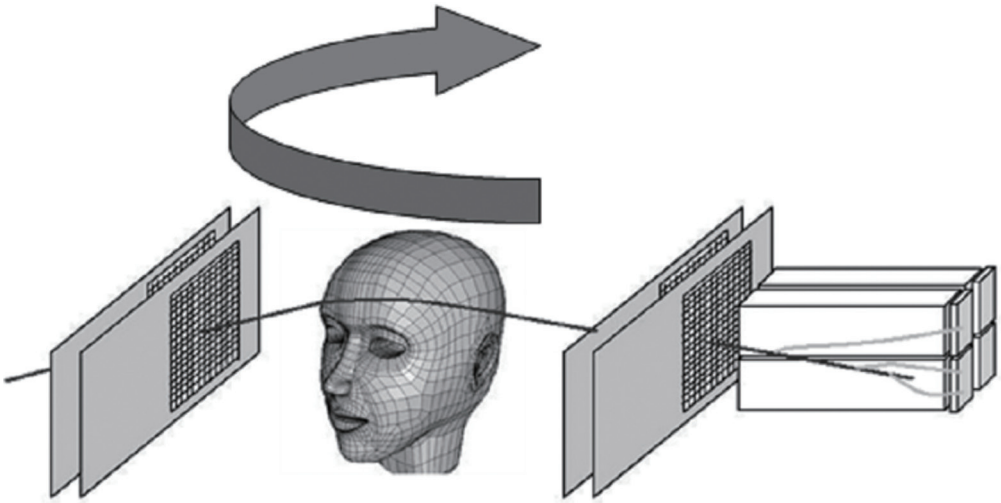

Figure 1 Schematic illustration of the first-generation pCT scanner. Protons are individually recorded by the four planes of position-sensitive silicon detectors which form the scanner reference system. These four planar detectors provide positions as well as angles of the protons in front and behind the object. A signal proportional to the energy of each outgoing proton is recorded with a segmented calorimeter in coincidence with its position and angle information. For a complete scan, the object is traversed by broad proton cone beam from many different projection angles

applied in HEP, allowed for the achievement of good spatial and energy resolution in the first generation prototype pCT scanner. For example, the silicon strip detectors in our Phase 1 scanner have a strip pitch of 228 μm, which allows to determine the position of protons at the level of each detector plane with better than 100 μm resolution. The crystal calorimeter has an intrinsic resolution of energy response of the order of 2%, which can be further improved by using a multi-stage plastic scintillator design in the Phase 2 scanner under construction.

Our conceptual approach to realizing pCT for treatment planning and image guidance originates from the approach described by Hanson *et al.* (28,29) and later work by Zygmanski *et al.* (30), although we deviate in some respect from these approaches, in particular in the implementation of reconstruction based on individual particle measurements. Our approach, outlined in more detail below, is based on a single-proton detection methodology; it uses a most likely path concept (24,27) to reconstruct along a curved path rather than a straight line, and iterative reconstruction algorithms to produce high-quality RSP reconstructions (31-33).

Proton CT offers the possibility to directly obtain the RSP distribution from proton energy measurements, which are then converted to a water equivalent pathlength (WEPL). Note that the WEPL of a proton through an object equals the line integral of RSP along the (not straight) proton path. With currently available detector technology, we have built the first generation of a pCT scanner whose design, originally proposed in (23) is shown in *Figure 1*. Individual protons are tracked before entering and after exiting the patient with two pairs of 2D sensitive silicon strip detectors (SSDs), providing information about proton position and direction at the boundaries of the image space. This allows the effects of multiple Coulomb scattering within the object to be accounted for in the estimation of an optimal trajectory or most likely path (MLP) (24,27).

In addition to tracking the position of individual protons, the energy lost by each proton after traversal of the image space is recorded in a calorimeter (an energy detector consisting of an array of cesium iodide (CsI) crystals). Using these measurements, one can obtain the WEPL, i.e., the path integral of relative stopping power along each path l, which is defined as

$$L = \int_l \rho dl \quad , \qquad [1]$$

where ρ is defined as the ratio of the local RSP of the tissue, S_{tissue}, to the RSP of water, S_{water}, thus

$$\rho = \frac{S_{\text{tissue}}}{S_{\text{water}}} \ . \qquad [2]$$

© Pioneer Bioscience Publishing Company. All rights reserved.

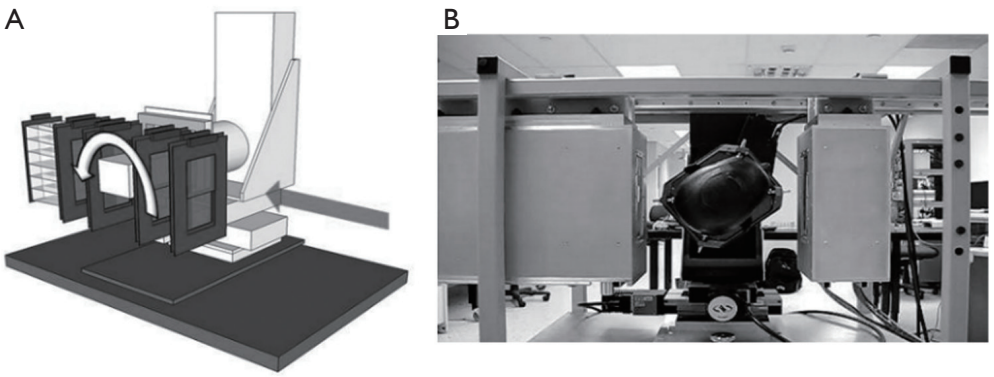

Figure 2 Schematic sketch (A) and view (B) of the first generation pCT scanner completed in 2011. The system consists of a front and rear module with a total of 4 silicon tracker planes and a crystal-calorimeter with an array of 18 CsI (Tl) crystals. The object (here a Rando head phantom) is rotating between the front- and rear-module on a precision rotational stage (Newport Corporation, Irvine, CA)

Assuming constant entry energy of the protons, the WEPL is strictly related to the energy of the outgoing protons. Thus, one can experimentally calibrate the scanner by relating the signal produced by the calorimeter to the WEPL of proton traversing a plate of polystyrene plates of known water-equivalent thickness, as recently described in (34).

In 2008, the Departments of Physics at Northern Illinois University and Radiation Medicine at LLUMC and the Santa Cruz Institute of Particle Physics (SCIPP) at UCSC received funding to build a Phase 1 preclinical head pCT scanner. The schematic layout of the Phase 1 pCT tracker and the device completed in 2011 are shown in *Figure 2*. It is comprised of front and rear SSD modules, consisting of 4 XY planes for full coordinate and direction data. The 18-crystal energy detector is integrated with the rear tracker modules. The scanner is mounted on a rail system that allows positioning of the detectors close to the phantom object that will rotate on a fixed, horizontal proton beam axis. The system also includes a precision microstage system for axial rotation and 3-axis translations. A more detailed description of this first generation pCT scanner can be found in (35).

The first generation pCT head scanner is not optimized for the high proton data rates that will be encountered in clinical operation. This is related to limitations of the data readout of the current data acquisition system and the rate limitations of the CsI energy detector. Another limitation is the relatively long image reconstruction time of up to 12 hours on conventional computing hardware. A third limitation of the Phase 1 scanner is its restricted sensitive area of 9 cm × 18 cm, which is suitable for head scans only.

The first 1.5 years of experience with the first generation scanner, which is currently mounted on one of the proton research beam lines at LLUMC, has shown that good quality RSP maps can be reconstructed but has also clearly demonstrated the technological limitations of this device. For example, *Figure 3* shows two RSP reconstructions obtained with the Lucy® phantom (Standard Imaging, Middleton, WI). The phantom consists of a 14-cm diameter polystyrene sphere that was equipped with cylindrical inserts of acrylic, bone-equivalent plastic, polystyrene, and air. As shown, spatial resolution has improved over time due to refinements in the reconstruction parameters, but also new artifacts have appeared which are related to differences in the responses of the different components of the CsI crystal matrix.

The Department of Radiation Medicine at LLUMC in collaboration with UCSC and the Department of Computer Science and Engineering at California State University San Bernardino (CSUSB) has received funding in 2011 to build the next generation pCT scanner, which will address the limitations of the first pCT scanner. The Department of Physics at Illinois University with Fermi National Accelerator Laboratory as collaborator has also received funding to build a Phase 2 scanner, albeit with somewhat different technology than the current Phase 1 scanner. A detailed description of the new scanner designs can be found in (36,37).

Figure 4 shows the schematic of the Phase 2 pCT scanner currently being built at LLUMC, CSUSB and UCSC. Without giving up the general concept shown in *Figure 1*, the LLUMC Phase 2 design will comprise a large-area silicon detector (9 cm by 36 cm) for the clinical pCT scanning with data acquisition rates increased by at least a

© Pioneer Bioscience Publishing Company. All rights reserved.

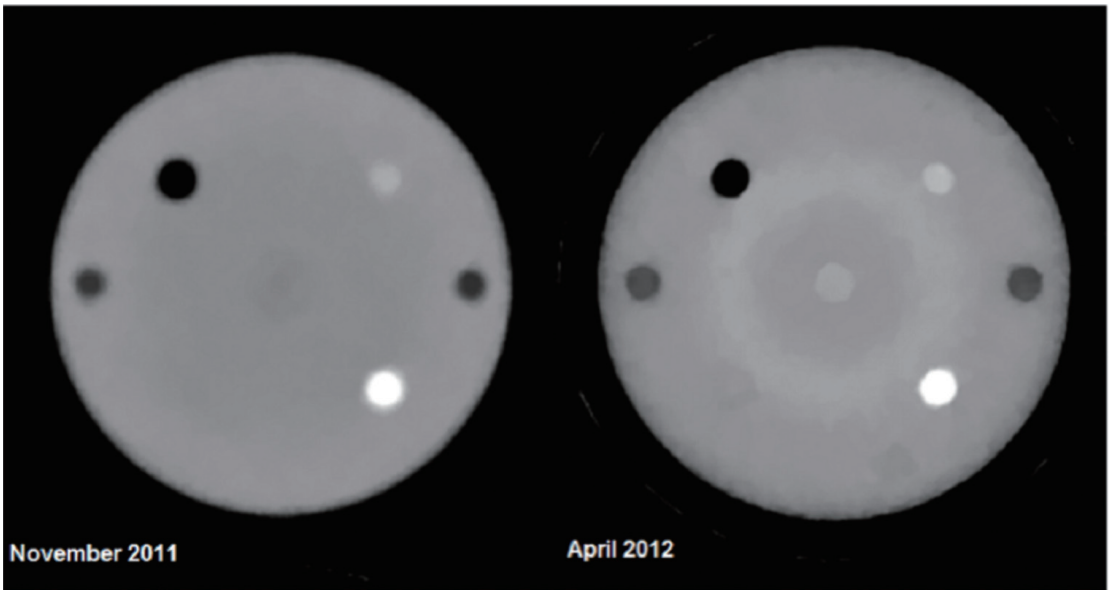

Figure 3 Cross sectional reconstructions of relative stopping power (RSP) of the Lucy® phantom through cylindrical inserts. The body of the Lucy sphere is made of polystyrene (RSP=1.035). The dark insert corresponds to air (RSP=0.05), the denser insert at the lower right to bone equivalent material (RSP=1.7), and the less dense insert in the upper right to acrylic (RSP=1.2). The right reconstruction, performed at a later time, shows improvement in resolution but also shows the presence of ring artifacts related to different responses of individual crystals in the calorimeter

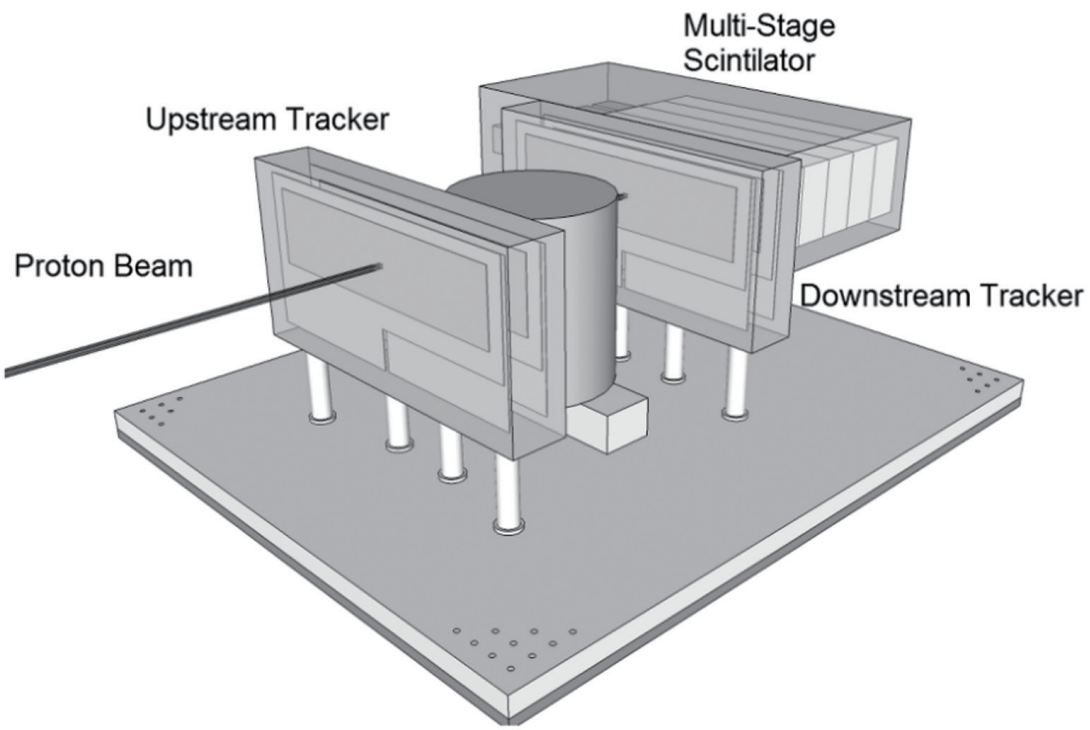

Figure 4 Schematic of the second generation (Phase 2) pCT scanner currently under construction. Different from Phase 1, the rotation stage is vertical rather than horizontal. The detector area will be expanded horizontally by a factor of two

© Pioneer Bioscience Publishing Company. All rights reserved.

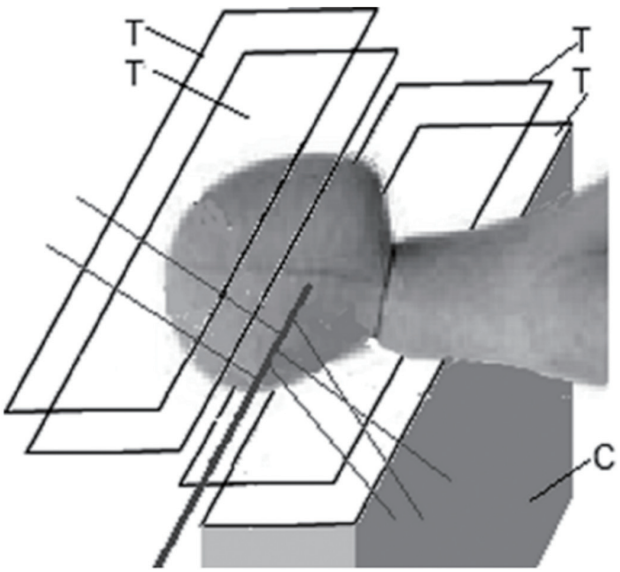

Figure 5 Principle of the large-angle scattered proton monitoring technique with two tracker telescopes with 4 position-sensitive planes (T). The protons scattered out of the primary beam (solid line) are detected by the trackers and their trajectory is back-tracked into the patient. The use of two telescopes increases the number of detected protons. With appropriate reconstruction techniques, the 3D position of the interaction points creating the scattered protons and thus the beam axis location can be inferred. In addition, one can also measure the energy of the tracked protons with a calorimeter (C) (here only shown in the lower half for clarity) to obtain additional data

factor of 10 from current rates to a sustained rate of about 2 MHz. The detectors will be mounted on a bread board with option of variable spacing relative to the phantom. The nominal distance between the inner silicon detectors will be 30 cm. The multi-segmented crystal energy detector will be replaced by a multi-stage scintillation (MSS) detector which has shown an intrinsic resolution of better than 1% in initial beam tests and provides a more uniform response.

After completion and acceptance testing of the Phase 2 pCT scanner, we will conduct a detailed performance evaluation of the pCT method using standard CT testing modules (Catphan® 600 phantom, The Phantom Laboratory, Inc., Salem, NY) including parameters such as image noise and noise power spectrum, field uniformity, high-contrast spatial frequency limits and modulation transfer function (MTF) measurements, low contrast detectability, and quantitative accuracy of CT numbers with materials of known RSP.

We will also evaluate the ability of the pCT scanning method to provide a more accurate proton range definition than currently possible with X-ray CT with a versatile proton range phantom, which will consist of a stack of radiochromic films (WET of 0.3 µm per film), embedded in the posterior fossa of a pediatric head phantom (CIRS). Proton pencil beams of known energy will be directed through different anatomical parts of the phantom and their observed range in the film stack will be compared to that predicted by pCT and X-ray CT-based treatment plans.

Large-angle proton scattering monitoring

Contemporary beam scanning nozzles contain monitors for the beam size, profile, position and beam intensity (38). The beam delivery control software receives signals from these beam monitors and frequently checks whether tolerances have been exceeded. Tolerance levels are generally much more stringent than for photon beam delivery, due to the sharpness of the rise and fall-off of dose in the Bragg peak. Since these monitors are located at considerable distance from the patient, the required accuracy of beam position is difficult to achieve. Very small deviations in the beam position at detector level can lead to relatively large deviations in the patient. In addition, there is no exact knowledge about loss of energy and intensity in beam modifying devices and immobilization devices that are located downstream from the monitoring detectors. Therefore, it would be very attractive to develop methods that allow for *online* monitoring of all relevant beam parameters as the beam enters and interacts with the patient.

Detecting and reconstructing the origin of large-angle scattered protons from primary proton pencil beams is a novel method investigated for fast and accurate proton beam monitoring. The principle, schematically shown in *Figure 5*, is based on the detection of distinct protons that are scattered out of primary beam due to elastic or inelastic nuclear interactions within the patient. A significant number of these scattered protons will be energetic enough to leave the patient, and their properties can be measured with particle detectors developed for pCT. Fast reconstruction of scattered proton tracks and their origin will primarily allow monitoring of beam position and size; the intensity of scattered protons will correlate with the primary beam intensity and energy, and hence these parameters could also be monitored with this technique.

First experiments demonstrating the potential of this

© Pioneer Bioscience Publishing Company. All rights reserved.

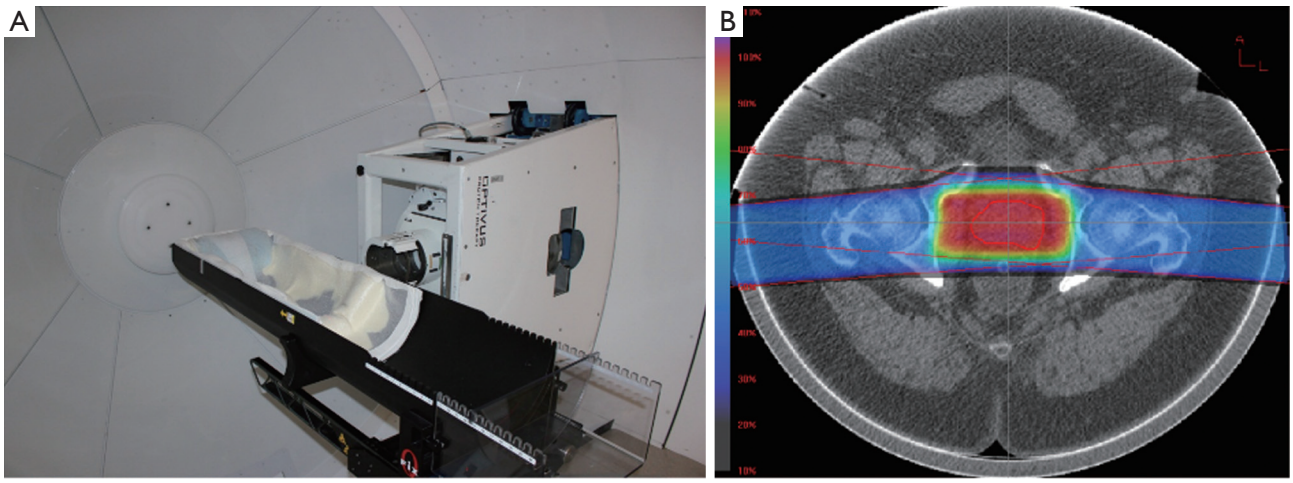

Figure 6 A pod immobilization system mounted to a six-degree of freedom robotic patient positioner at LLUMC (A); example of how pod immobilization maintains a consistent patient external contour minimizing the impact of the contour on range uncertainty (B)

monitoring technique were performed at the LLUMC proton treatment center and were presented at the 2008 IEEE Nuclear Science Symposium (39). A human head phantom was irradiated with 250 and 100 MeV proton pencil beams, and scattered protons were detected with a silicon microstrip tracker located near the phantom. Extrapolation of about 10^4 scattered proton tracks back to a focus plane inside the phantom demonstrated the feasibility of reconstructing the location of the pencil beam and estimating its axis inside the phantom with sub-millimeter accuracy. Although the slow readout system of the pCT tracker used in these first experiments did not permit measurement of the actual flux of the scattered protons, subsequent Geant4 Monte Carlo simulations of the experiment indicated that with fast and efficient particle detectors one could register 10^6-10^7 scattered protons per single proton beam spill of 10^{10} primary protons (33).

An additional preliminary feasibility test of the proton scattering monitoring technique was carried out at the LLUMC proton center using the Phase 1 proton CT scanner (see above). In particular, a phantom, consisting of a PMMA cylinder of 15 cm diameter filled with water, was exposed to 126 and 200 MeV proton pencil beams. Protons emerging from the phantom at 90 degrees with respect to the direction of the incoming beam were tracked in the four planes of silicon microstrip detectors of the scanner, while their energy was measured with the segmented CsI calorimeter. The beam position and its profile in the vertical plane were reconstructed by extrapolating the trajectories of reconstructed protons back to their point of origin along the beam axis. Using a sample of 11,500 reconstructed tracks from data taken with the 200 MeV beam, the vertical beam position was determined with a statistical accuracy of 0.07 mm and a realistic beam width of 3.60±0.11 mm was determined from the reconstructed vertical beam profile. The results of this test, though very limited in scope and event statistics, highlight the promising perspectives of the proposed technique.

Advances in proton immobilization

Immobilization is not a new concept in radiation therapy as it has been used over the years in photon and electron therapy to place the patient in a reproducible and stable position for treatment. This is no different in proton therapy, as the use of both external and internal immobilization impacts the ability to cover a target with the specific treatment dose. However, unlike in photon therapy, the third dimension of depth is very critical in proton beam delivery. Changes in patient contour or target position along the beam axis can impact the position of the distal edge of the Bragg peak relative to the tumor. Pod immobilization (see *Figure 6*) has been used extensively at LLUMC over the past 20 years in order to not only provide superior body immobilization but also control the reproducibility of the patient's external contour, especially on larger patients, hence removing a source of range uncertainty which can impact Bragg peak placement.

© Pioneer Bioscience Publishing Company. All rights reserved.

Figure 7 CT images of immobilization devices whose heterogeneity and lack of part-to-part reproducibility makes them unsuitable for proton therapy immobilization

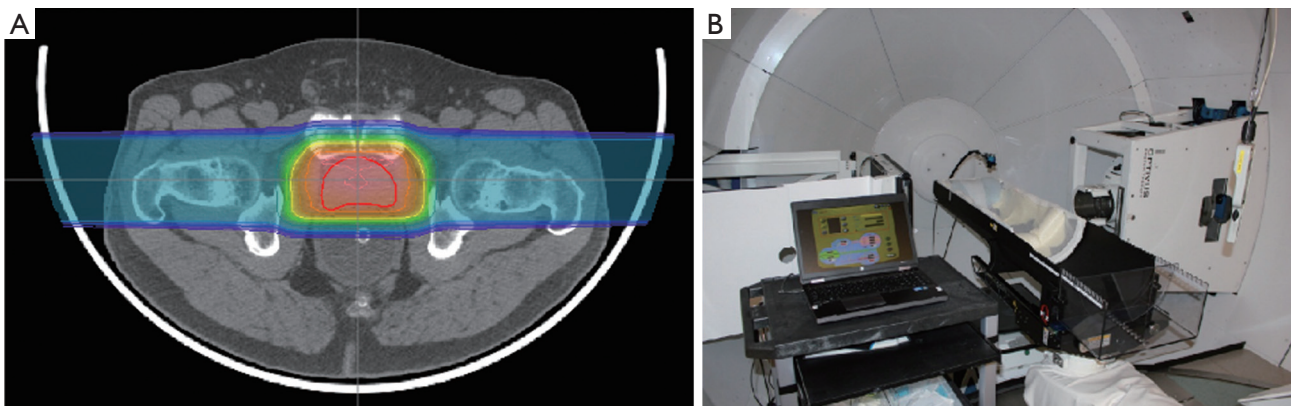

Figure 8 A. A proton prostate plan which utilizes a water-filled endo-rectal balloon to limit prostate motion during and between treatments; B. example of a spirometric device that assists in deep-inspiration breath-hold treatment delivery at LLUMC

It is important to realize that the distal edge placement of each proton beam is modified by any device placed upstream (closer to the beam source) of the patient, including immobilization devices. It is imperative that such devices are taken into account accurately by the treatment planning system, and that their water equivalent thickness (WET) is known precisely and verified using measured proton data. Devices that are non-uniform may change their internal composition between the time of the initial imaging for treatment planning and the time of patient treatment; similar attention must be paid to differences in the materials used for the purposes of planning and treatment delivery (*Figure 7*). Prior to clinical implementation all immobilization devices should be thoroughly evaluated including CT imaging, treatment planning system evaluation and measured WET data to ensure that the impact of the devices on the treatment process is understood.

Bragg peak placement is controlled using a range shifter in passive proton beam delivery or through dynamic changes in proton energy for active proton delivery. Regardless of the beam delivery method, the Bragg peak placement is determined by the location (or water equivalent depth) of the target relative to upstream anatomy, including bony structures or air cavities. Motion of the target relative to these anatomical structures can cause a mismatch between the range shifter or energy selected and the target's water equivalent depth, leading to either over-irradiation of normal tissue past the target or under-irradiation of the target itself. To minimize this mismatch, inter- and intra-fraction motion must be minimized to ensure the target is in the same location at the time of treatment that it was during CT imaging and treatment planning. For example, in prostate treatments this can be accomplished by asking the patient to maintain a modestly full bladder during imaging and treatment, and by placing an endorectal balloon (*Figure 8A*), as shown by our recent and yet unpublished study of 25 consecutive prostate cancer patients. For structures that are influenced by respiratory motion, including liver and intra-abdominal tumors, advances in spirometric and optical tracking systems allow for reproducible beam delivery during the respiratory cycle (*Figure 8B*).

© Pioneer Bioscience Publishing Company. All rights reserved.

As more proton therapy centers come online, a good understanding of immobilization devices and how these will impact the proton dose profile and its accuracy is necessary to maintain treatment efficacy. Centers using more than one radiation modality (e.g., protons and photon IMRT) also need to consider the functionality of their current immobilization devices and whether these devices are suited to proton therapy. Immobilization devices specifically developed for proton therapy may be the best solution in theory, but may prove too costly to maintain and place unnecessary burdens on staff training in practice. Further, immobilization devices used exclusively for proton therapy may limit use of other radiation modalities in patients that receive combined-modality treatments, as they require re-immobilization and re-scanning of patients as they are moved from one to the next treatment modality. As such, immobilization solutions that meet the needs of both the photon and proton treatment modalities should be considered, allowing for maximum treatment flexibility, while maintaining adequate patient immobilization.

Discussion and conclusions

Proton therapy is still an evolving radiation therapy modality. With an increasing number of patients treated worldwide, technological advancements in proton therapy are likely to occur at an increasing pace.

Range uncertainties due to tissue and immobilization device material heterogeneity and stopping power uncertainties are important challenges to overcome in proton therapy, in particular, if targets in moving and deformable organs are treated and more hypofractionated treatment protocols are being investigated in the clinic.

Reducing range uncertainties will support the development of clinical protocols based on inversely planned IMPBT. The IMPBT technology has additional challenges that will need input from multidisciplinary teams. We have proposed and are currently testing a new method for monitoring proton pencil beam delivery during active beam scanning, which is based on detecting large-angle scattered protons arising from the primary beam. Similar and complementary monitoring techniques using prompt gamma detection and post-treatment monitoring of positron emitter distribution created by nuclear interactions during treatment are likely to be further developed and integrated in the treatment room environment.

Suitable immobilization devices and techniques are also likely to continue to evolve. Rather than adopting existing devices and techniques that have been developed for primary application in photon radiation therapy, focus needs to shift to devices that address the special demands of charged particle therapy. Ideally, these devices will be part of a universal immobilization suite that can be employed for multi-modality treatments utilizing both proton and photon irradiation. Rather than focusing on proton beam gating, we believe that internal organ and tumor motion is best controlled by devices that restrict this motion and stabilize the treated organ. Therefore, we prefer the use of passive devices such as an endorectal balloon for prostate treatments and active breathing control in patients undergoing lung and abdominal proton therapy.

We have presented examples of ongoing translational research and development in proton therapy that are also applicable to carbon ion therapy. Forming research relationships with open exchange of ideas and research results is, in our opinion, the key to accelerated progress in this field. Appropriate technology transfer protocols should be developed that allow an efficient transition from the research environment to clinical application.

Summary

Charged particle therapy with protons and heavy ions started almost 60 years ago, but continues to evolve clinically and technologically. Important aspects that need to be addressed include the reduction of proton range uncertainty, the development of active beam scanning technology and its monitoring, and advanced immobilization techniques that take the special requirements of charged particle beams into account. Translational research activities are presented that focus on these areas.

Acknowledgements

The authors are supported by Grant No. 1R01EB013118-01 from the Institute of Biomedical Imaging and Bioengineering at the National Institutes of Health. The content of this paper is solely the responsibility of the authors and does not necessarily represent the official views of the National Institute of Biomedical Imaging and Bioengineering or the National Institutes of Health. The first author would also like to acknowledge financial support received by the United States - Israel Binational Science Foundation (BSF), grant Number 2009012. The Phase 1 proton CT development was partially funded by the U.S. Department of Defense Prostate Cancer Research Program Award No.

© Pioneer Bioscience Publishing Company. All rights reserved.

W81XWH-12-1-0122 to Northern Illinois University and the Department of Radiation Medicine.

Disclosure: This manuscript has not been submitted or published elsewhere. The authors have no potential conflicts of interest related to the information contained herein.

References

1. Particle therapy facilities in operation. Particle Therapy Co-Operative Group. Available online: http://ptcog.web.psi.ch/ptcentres.html
2. Allen AM, Pawlicki T, Dong L, et al. An evidence based review of proton beam therapy: the report of ASTRO's emerging technology committee. Radiother Oncol 2012;103:8-11.
3. Lomax AJ. Intensity modulated proton therapy and its sensitivity to treatment uncertainties 1: the potential effects of calculational uncertainties. Phys Med Biol 2008;53:1027-42.
4. Jiang H, Seco J, Paganetti H. Effects of Hounsfield number conversion on CT based proton Monte Carlo dose calculations. Med Phys 2007;34:1439-49.
5. España S, Paganetti H. The impact of uncertainties in the CT conversion algorithm when predicting proton beam ranges in patients from dose and PET-activity distributions. Phys Med Biol 2010;55:7557-71.
6. Paganetti H. Range uncertainties in proton therapy and the role of Monte Carlo simulations. Phys Med Biol 2012;57:R99-117.
7. Gensheimer MF, Yock TI, Liebsch NJ, et al. In vivo proton beam range verification using spine MRI changes. Int J Radiat Oncol Biol Phys 2010;78:268-75.
8. Chen W, Unkelbach J, Trofimov A, et al. Including robustness in multi-criteria optimization for intensity-modulated proton therapy. Phys Med Biol 2012;57:591-608.
9. Unkelbach J, Bortfeld T, Martin BC, et al. Reducing the sensitivity of IMPT treatment plans to setup errors and range uncertainties via probabilistic treatment planning. Med Phys 2009;36:149-63.
10. Unkelbach J, Chan TC, Bortfeld T. Accounting for range uncertainties in the optimization of intensity modulated proton therapy. Phys Med Biol 2007;52:2755-73.
11. Yang M, Virshup G, Clayton J, et al. Theoretical variance analysis of single- and dual-energy computed tomography methods for calculating proton stopping power ratios of biological tissues. Phys Med Biol 2010;55:1343-62.
12. Urie M, Goitein M, Wagner M. Compensating for heterogeneities in proton radiation therapy. Phys Med Biol 1984;29:553-66.
13. Chen GT, Singh RP, Castro JR, et al. Treatment planning for heavy ion radiotherapy. Int J Radiat Oncol Biol Phys 1979;5:1809-19.
14. Schneider U, Pedroni E. Proton radiography as a tool for quality control in proton therapy. Med Phys 1995;22:353-63.
15. Schneider U, Pedroni E, Lomax A. The calibration of CT Hounsfield units for radiotherapy treatment planning. Phys Med Biol 1996;41:111-24.
16. International Commission of Radiation Units and Measurements. Tissue Substitutes in Radiation Dosimetry and Measurements. ICRU Report 44, ICRU, Bethesda, MD, 1989.
17. Schneider U, Pemler P, Besserer J, et al. Patient specific optimization of the relation between CT-hounsfield units and proton stopping power with proton radiography. Med Phys 2005;32:195-9.
18. Cormack AM. Representation of a function by its line integrals, with some radiological applications. Jour Appl Phys 1963;34:2722-7.
19. Allan M. Cormack, Godfrey N. Hounsfield. The Nobel Prize in Physiology or Medicine 1979. Available online: http://nobelprize.org/nobel_prizes/medicine/laureates/1979/cormack-lecture.html
20. Sipala V, Bruzzi M, Bucciolini M, et al. A proton imaging device: Design and status of realization. Nucl Instrum Methods A 2010;612:566-70.
21. Sadrozinski HF-W, Bashkirov V, Bruzzi M, et al. Issues in proton computed tomography. Nucl Instrum Methods A 2003;511:275-81.
22. Johnson LR, Keeney B, Ross G, et al. Initial studies on proton computed tomography using a silicon strip detector telescope. Nucl Instrum Methods A 2003;514:215-23.
23. Schulte RW, Bashkirov V, Li T, et al. Conceptual design of a proton computed tomography system for applications in proton radiation therapy. IEEE Trans Nuc Sci 2004;51:866-72.
24. Williams DC. The most likely path of an energetic charged particle through a uniform medium. Phys Med Biol 2004;49:2899-911.
25. Schulte RW, Bashkirov V, Klock MC, et al. Density resolution of proton computed tomography. Med Phys 2005;32:1035-46.
26. Li T, Liang Z, Singanallur JV, et al. Reconstruction for proton computed tomography by tracing proton trajectories: a Monte Carlo study. Med Phys 2006;33:699-706.
27. Schulte RW, Penfold SN, Tafas JT, et al. A maximum

© Pioneer Bioscience Publishing Company. All rights reserved.

likelihood proton path formalism for application in proton computed tomography. Med Phys 2008;35:4849-56.
28. Hanson KM, Bradbury JN, Cannon TM, et al. Computed tomography using proton energy loss. Phys Med Biol 1981;26:965-83.
29. Hanson KM, Bradbury JN, Koeppe RA, et al. Proton computed tomography of human specimens. Phys Med Biol 1982;27:25-36.
30. Zygmanski P, Gall KP, Rabin MS, et al. The measurement of proton stopping power using proton-cone-beam computed tomography. Phys Med Biol 2000;45:511-28.
31. Penfold SN, Rosenfeld AB, Schulte RW, et al. A more accurate reconstruction system matrix for quantitative proton computed tomography. Med Phys 2009;36:4511-8.
32. Penfold SN, Schulte RW, Censor Y, et al. Total variation superiorization schemes in proton computed tomography image reconstruction. Med Phys 2010;37:5887-95.
33. Penfold SN. Image reconstruction and Monte Carlo simulations in the development of proton computed tomography for applications in proton radiation therapy. Ph.D. thesis, University of Wollongong, 2010.
34. Hurley RF, Schulte RW, Bashkirov VA, et al. Water-equivalent path length calibration of a prototype proton CT scanner. Med Phys 2012;39:2438-46.
35. Hurley RF, Schulte RW, Bashkirov VA, et al. The phase I proton CT scanner and test beam results at LLUMC. T Am Nucl Soc 2012;106:63-66.
36. Schulte RW, Bashkirov V, Johnson R, et al. T Am Nucl Soc 2012;106:59-62.
37. Zutshi V. Overview of the NIU/Fermilab Phase 2 proton CT project. T Am Nucl Soc 2012;106:67-68.
38. Flanz J. Particle Beam Scanning. In: Paganetti H. eds. Proton Therapy Physics. Boca Raton, FL: CRC Press/ Taylor & Francis, 2011:158-89.
39. Bashkirov VA. Proton Computed Tomography: a Status Update. Presented at the Special Focus Workshop: Innovative Techniques for Hadron Therapy. 2008 IEEE Nuclear Science Symposium, Medical Imaging Conference.

Cite this article as: Schulte RW, Wroe AJ. New developments in treatment planning and verification of particle beam therapy. Transl Cancer Res 2012;1(3):184-195. DOI: 10.3978/j.issn.2218-676X.2012.10.07

© Pioneer Bioscience Publishing Company. All rights reserved.